Fecal microbiota transplantation plus tislelizumab and fruquintinib in refractory microsatellite stable metastatic colorectal cancer: an open-label, single-arm, phase II trial (RENMIN-215)

Wensi Zhao,[a] Jun Lei,[a] Shaobo Ke,[a] Yuan Chen,[b] Jiping Xiao,[c] Ze Tang,[d] Li Wang,[e] Yiping Ren,[f] Mohammed Alnaggar,[g] Hu Qiu,[a] Wei Shi,[a] Lei Yin,[h,**] and Yongshun Chen[a,*]

[a]Department of Clinical Oncology, Renmin Hospital of Wuhan University, Wuhan, China
[b]Department of Clinical Oncology, Qianjiang Central Hospital, Qianjiang, China
[c]Department of Abdominal Tumor Surgery, Huangshi Central Hospital, Affiliated Hospital of Hubei Polytechnic University, Huangshi, China
[d]Department of Abdominal & Pelvic Medical Oncology, Huangshi Central Hospital, Affiliated Hospital of Hubei Polytechnic University, Huangshi, China
[e]Department of Oncology, Xiaochang First People's Hospital, China
[f]Department of Clinical Oncology, Jingshan Union Hospital of Huazhong University of Science and Technology, Jingshan, China
[g]Department of Internal Medicine, Clinic Medical College, Hubei University of Science and Technology, Xianning, China
[h]State Key Laboratory of Virology, Hubei Key Laboratory of Cell Homeostasis, College of Life Sciences, Wuhan University, Wuhan, China

eClinicalMedicine 2023;66: 102315

Published Online xxx https://doi.org/10.1016/j.eclinm.2023.102315

Summary

Background Immunotherapy has revolutionized the treatment of cancer. However, microsatellite stable (MSS) metastatic colorectal cancer (mCRC) shows a low response to PD-1 inhibitors. Antiangiogenic therapy can enhance anti-PD-1 efficacy, but it still cannot meet clinical needs. Increasing evidence supported a close relationship between gut microbiome and anti-PD-1 efficacy. This study aimed to explore the efficacy and safety of the combination of fecal microbiota transplantation (FMT) and tislelizumab and fruquintinib in refractory MSS mCRC.

Methods In the phase II trial, MSS mCRC patients were administered FMT plus tislelizumab and fruquintinib as a third-line or above treatment. The primary endpoint was progression-free survival (PFS). Secondary endpoints were overall survival (OS), objective response rate (ORR), disease control rate (DCR), duration of response (DoR), clinical benefit rate (CBR), safety and quality of life. Feces and peripheral blood were collected for exploratory biomarker analysis. This study is registered with Chictr.org.cn, identifier ChiCTR2100046768.

Findings From May 10, 2021 to January 17, 2022, 20 patients were enrolled. Median follow-up was 13.7 months. Median PFS was 9.6 months (95% CI 4.1–15.1). Median OS was 13.7 months (95% CI 9.3–17.7). Median DoR was 8.1 months (95% CI 1.7–10.6). ORR was 20% (95% CI 5.7–43.7). DCR was 95% (95% CI 75.1–99.9). CBR was 60% (95% CI 36.1–80.9). Nineteen patients (95%) experienced at least one treatment-related adverse event (TRAE). Six patients (30%) had grade 3–4 TRAEs, with the most common being albuminuria (10%), urine occult blood (10%), fecal occult blood (10%), hypertension (5%), hyperglycemia (5%), liver dysfunction (5%), hand-foot skin reaction (5%), and hypothyroidism (5%). No treatment-related deaths occurred. Responders had a high-abundance of *Proteobacteria* and *Lachnospiraceae* family and a low-abundance of *Actinobacteriota* and *Bifidobacterium*. The treatment did not change the structure of peripheral blood TCR repertoire. However, the expanded TCRs exhibited the characteristics of antigen-driven responses in responders.

Interpretation FMT plus tislelizumab and fruquintinib as third-line or above treatment showed improved survival and manageable safety in refractory MSS mCRC, suggesting a valuable new treatment option for this patient population.

Funding This study was supported by the National Natural Science Foundation of China (82102954 to Wensi Zhao) and the Special Project of Central Government for Local Science and Technology Development of Hubei Province (ZYYD2020000169 to Yongshun Chen).

*Corresponding author. Cancer Center, Renmin Hospital of Wuhan University, 238 Jiefang Road, Wuchang District, Wuhan, 430060, China.
**Corresponding author. State Key Laboratory of Virology, Department of Biochemistry and Molecular Biology, Hubei Key Laboratory of Cell Homeostasis, College of Life Science, Wuhan University, Wuhan, 430072, China.
E-mail addresses: yongshun2007@163.com (Y. Chen), yinlei@whu.edu.cn (L. Yin).

Keywords: Metastatic colorectal cancer; Microsatellite stable; Fecal microbiota transplantation; Tislelizumab; Fruquintinib

Research in context

Evidence before this study

We searched PubMed and major oncology congresses (the ASCO, ASCO-GI, ESMO and ESMO-IO) for studies on ICI-based therapies for mCRC until July 10, 2023, using search terms of "metastatic colorectal cancer", "immunotherapy", "anti-PD-1", "anti-PD-L1", "VEGFR", "anti-angiogenesis", "gut microbiome", "fecal microbiota transplantation", "immuno-resistance" and "progressed", without language restriction. TKIs plus ICIs gained varying success in MSS CRC including REGONIVO, LEAP-005 and REGOMUNE trials. However, efficacy of TKI in combination with ICI remains limited. Gut microbiome was reported to improve the antitumor immunity and promote response to ICIs. Two phase I trials showed that anti-PD-1 resistance can be overcome by inducing gut microbiota perturbations via FMT, resulting in rapid and durable clinical benefit for some melanoma patients.

Added value of this study

This phase II study showed that FMT plus tislelizumab and fruquintinib demonstrated a promising antitumor activity and controllable safety in refractory MSS mCRC. How to improve survival without compromising patients' quality of life is something we are always exploring. Here, FMT plus ICI and TKI stands for a rational and novel strategy in the era of chemo-free for MSS mCRC patients.

Implications of all the available evidence

Our study provides further evidence of the clinical activity and safety of FMT plus tislelizumab and fruquintinib as third-line or above treatment in refractory MSS mCRC. High *Lachnospiraceae* abundance in fecal and expanded TCRs in peripheral blood may be valuable classifiers for prognosis prediction and risk stratification.

Introduction

Colorectal cancer (CRC) ranks in the top three most common cancers worldwide and in the top two in terms of mortality, with 1,931,590 new cases and 935,173 deaths estimated in 2020.[1] In the metastatic setting, fluorouracil based doublet or triplet chemotherapy combined with anti-vascular endothelial growth factor (VEGF) or anti-epidermal growth factor receptor (EGFR) targeted therapy are the globally recognized standard of first- and second-line treatments.[2–4] However, the currently available third-line or above treatment options are limited, including only regorafenib and TAS-102 plus bevacizumab, either provide unsatisfactory disease control or have a relatively high incidence of treatment-related adverse events (TRAEs).[5–7] There is therefore a pressing clinical need for effective later-line treatment for metastatic CRC (mCRC).

The addition of immune checkpoint inhibitors (ICIs) has significantly revolutionized the treatment landscape for the vast majority of cancers.[8–12] ICIs have been preferentially recommended for mismatch repair-deficient (dMMR) or microsatellite instability-high (MSI-H) tumors, including CRC. However, in mCRC, only about 5% of patients were dMMR/MSI-H phenotype. The mismatch repair-proficient or microsatellite-stable (pMMR/MSS) CRC patients, which accounts for the majority of the cases, showed little respond to ICIs due to the immunosuppressive tumor microenvironment.

Rational treatment combinations have been extensively explored. Clinical data indicated a potential synergistic effect of ICIs combined with anti-angiogenetic therapy in MSS mCRC who failed or had disease progressed after prior oxaliplatin- and irinotecan-based standard treatments. Regorafenib plus nivolumab yielded an ORR of 33% and mPFS of 7.9 months in advanced MSS CRC patients.[13] Regorafenib plus toripalimab showed an ORR of 15.2%, mPFS of 2.1 months and mOS of 15.5 months in MSS mCRC patients.[14]

Fruquintinib, a highly selective small-molecule tyrosine kinase inhibitor (TKI) of VEGFR-1, -2, and -3, was approved by the China National Medical Products Administration for third-line treatment of mCRC based on the FRESCO study with mPFS of 3.7 months and mOS of 9.3 months.[15] Fruquintinib plus sintilimab resulted an ORR of 20.9% and DCR of 88.4% with the mPFS of 5.6 months and mOS of 14.3 months in mCRC patients who had failed standard treatment.[16] Despite some improvement, the efficacy of TKIs in combination with ICIs, in general, remains limited.

It was reported that the gut microbiome of immunotherapy-sensitive patients was distinct from that of immuno-resistant populations.[17] Certain gut bacteria contributed to the better immune response.[18] Regulating the composition of gut microbiota can enhance the anti-PD-1 immunotherapy efficacy.[19–21] Results from two phase I trials showed that responder-

derived fecal microbiota transplantation (FMT) effectively reversed the immuno-resistance in melanoma, laying the foundation for the clinical application of FMT to reprogram the tumor microenvironment (TME) in cancer immunotherapy.[22,23]

Tislelizumab is a humanized IgG4 monoclonal antibody (mAb) against PD-1 with high affinity and specificity. It was engineered to minimize binding to FcγR on macrophages to greatly reduce antibody dependent phagocytosis, a potential mechanism of T-cell clearance and resistance to anti-PD-1 therapy.[24,25]

Herein, we evaluated the safety, quality of life, efficacy, and efficacy-related gut microbiome and peripheral blood TCR features of FMT in combination with tislelizumab and fruquintinib in mCRC patients with MSS/pMMR phenotype in third-line or above settings.

Methods

Study design and participants

The present study is an open-label, single-arm, phase II trial performed at the Renmin Hospital of Wuhan University in China to evaluate the efficacy and safety of the combination of fecal microbiota transplantation with tislelizumab and fruquintinib as third-line or above therapy in mCRC patients with MSS/pMMR phenotype.

Eligible patients were aged ≥18 years with histologically confirmed metastatic, or progressive MSS/pMMR CRC, progression (radiologically or clinically) or intolerance to at least second-line systemic chemotherapy, at least one measurable lesion according to Response Evaluation Criteria in Solid Tumors (RECIST v1.1), an Eastern Cooperative Oncology Group performance status (ECOG PS) of 0–2; and adequate hematologic, hepatic, and renal function. Microsatellite status was performed by immunohistochemistry and/or polymerase chain reaction and next-generation sequencing. Major exclusion criteria included a history of or active autoimmune disease, a concomitant second cancer, history of organ transplantation or any form of immunotherapy, or ongoing systemic immunosuppressive therapy, any factors affecting oral drug absorption. Full inclusion and exclusion criteria are listed in the protocol (online only). The manuscript adheres to CONSORT reporting guidelines.

Procedures

Before receiving FMT, patients underwent an initial "native microbiota depletion" phase (Days −3 to −1) in which they were administered with orally ingested antibiotics (vancomycin 500 mg and neomycin 100 mg q6 hours) for 72 h. During last 15 h, oral PEG-based diarrhea solution (inulin fructo-oligosaccharide powder) was used for intestinal cleansing preparation and flora colonization. FMT was then performed via administration of oral custom-made stool capsules (capsulized FMT) at a dose of 30 capsules/day (equivalent to 3 bottles of 40 mL liquid intestinal microecological preparations) for 3 consecutive days on a 3-week cycle.

Fruquintinib was administered orally once daily at a starting dose of 5 mg for 2 weeks on/1 week off and tislelizumab 200 mg was administered intravenously once every 3 weeks, until unacceptable toxicities, loss of clinical benefit, disease progression, death, completion of 18 cycles of study treatment, or at the patient's request. Protocol-defined dose modifications to manage treatment-related toxicity included interruption of fruquintinib and tislelizumab, and reducing the fruquintinib dose from 5 mg to 4 mg daily or further to 3 mg daily. No dose adjustments were allowed for tislelizumab.

Endpoints

All participants who received at least one dose of study intervention were included in the efficacy and safety analyses. Peripheral blood and stool specimens were obtained serially for biomarkers and gut microbiome analyses.

Tumor responses were assessed by independent radiologists according to Response Evaluation Criteria in Solid Tumors (RECIST) v1.1 at baseline, every two cycles in the first year, and every 3 months thereafter until disease progression (PD) or the end of the study. Adverse event (AE) data were collected according to the Medical Dictionary for Regulatory Activities v23.0, and the severity was graded using the National Cancer Institute Common Terminology Criteria for Adverse Events v5.0. AE data were collected up to 30 days after treatment discontinuation, immune-related AE (irAE) data were collected up to 90 days after the last dose of tislelizumab. Treatment continued until unacceptable toxicity, the investigator's decision, withdrawal of consent, study completion, or death. For a patient with initial radiological disease progression (i.e., no clinical deterioration), if the investigator judged that the patient would benefit from and were tolerant of continued treatment, and if the patient had been informed and provided voluntary consent, the treatment was allowed to continue.

The primary end point was the progression-free survival (PFS). The secondary end points included overall survival (OS), objective response rate (ORR), disease control rate (DCR), duration of response (DoR), clinical benefit rate (CBR), safety and quality of life evaluation. Complete response (CR), partial response (PR), stable disease (SD) or PD was required to be confirmed at least 4 weeks later. Outcomes of T cell receptor (TCR) sequencing from peripheral blood mononuclear cells (PBMCs) and 16S rDNA amplicon pyrosequencing from stool bacterial genomic DNA samples were evaluated as prespecified exploratory endpoints.

Statistics

This study was designed to have a power of 80% to detect an increase in the mPFS from 3.7 months of PD-

1 inhibitor monotherapy and/or anti-VEGFR TKI in third-line or above setting to a target of 7.6 months (Supplementary Table S1), with a one-sided type I error of 0.025 in favor of the combination of anti-PD-1 plus anti-VEGFR and FMT. Patients were accrued for a period of 12 months and the follow-up continued for a period of 24 months after the last patient was added. Considering an estimated 5% dropout rate, a total of 19 patients were needed.

The PFS, DoR, and OS were plotted using the Kaplan–Meier method. The log-rank test was used to compare Kaplan–Meier curves, and Cox proportional hazards model was adopted to determine the hazard ratio (HR) and its associated bilateral 95% CI and *P* value. The assumption of proportional hazards in the Cox analysis was assessed first by testing statistical significance of interactions between follow-up time and exposures. With any covariate violating the assumption, we added their interaction with time to the model. Scatter plot of independent variable and martingale residual established by R to test the linear relationship of each covariate in the Cox model. For the ORR, DCR, CBR and 95% confidence intervals, despite conservatism, the exact Clopper-Pearson method was used to compute binomial CIs of each single rate due to the small sample size. The association of clinical characteristics with response was estimated via logistic regression and compared between groups by using Fisher's exact test or chi-square test, as appropriate. Other clinical outcomes, demographic characteristics, and safety were summarized descriptively. All statistical analyses were performed using SPSS v26.0. Bioinformatics analyses of sequence data were mainly performed using QIIME2 version 2022.2, R version 3.2.0 and Bioconductor version 2.14.

Ethics

The study was conducted in accordance with the Declaration of Helsinki, the International Conference on Harmonization Guidelines for Good Clinical Practice, and applicable local regulations. The protocol was reviewed and approved by the Ethics Committee of the Renmin Hospital of Wuhan University (Approval Number: WDRY2021-K049), and registered on Chictr. org.cn (identifier: ChiCTR2100046768). All patients provided written informed consent before study entry.

Role of the funding source

The funder of the study had no role in study design, data collection, data analysis, data interpretation, or writing of the manuscript. All authors verified that this study was done according to the protocol and was attested for data accuracy and completeness. All authors had full access to all of the data in the study and accepted responsibility for the decision to submit the final manuscript for publication.

Results

Participants

Between May 10, 2020, and January 17, 2022, a total of 31 patients were screened, of whom 20 eligible patients were enrolled for eligibility and received at least one dose of the study regimen (ITT and safety set; Fig. 1). All patients completed the first scheduled post-baseline tumor assessment. The treatment responses were evaluated as shown in Fig. 2.

Patients were predominantly males (90%), with a median age of 62 years (range, 42–79). Of the 20 patients enrolled, 16 (80%) had an ECOG PS of 1; 14 (70%) had primary tumor at left-side colon and rectum; 14 (70%) had liver metastasis. All patients received at least second-line of prior systemic therapy, with 11 (55%) receiving ≥3 lines. Among them, 14 (70%) had previously administrated with anti-VEGF/VEGFR therapy (e.g., bevacizumab, regorafenib, or apatinib) and 9 (45%) had received prior local radioactive intervention. Gene mutation information was available for 16 patients (80%), and 7 (35%) were KRAS mutant type. All patients had MSS and/or pMMR phenotypes. The baseline characteristics of patients were presented in Table 1. The correlation between treatment response and patient characteristics and peripheral blood indicators was shown in Supplementary Table S2.

Efficacy

As of data cutoff on July 10, 2023, with a median follow-up of 13.7 months (range, 4.9–26.0), the median PFS was 9.6 months (95% CI 4.1–15.1) and median OS was 13.7 months (95% CI 9.3–17.7) (Fig. 3). Patients were labeled with responders (PFS ≥ 6 months; n = 12) and non-responders (PFS < 6 months; n = 8) and the CBR reached 60% (95% CI 36.1–80.9). The median treatment duration was 7.5 cycles (range 3–18 cycles) and the size of target lesion was reduced in 60% of patients (Fig. 4). In the ITT population, 4 patients achieved PR, 15 patients achieved SD, the ORR was 20% (95% CI 5.7–43.7), the DCR was 95% (95% CI 75.1–99.9). Median DoR was 8.1 months (95% CI 1.7–10.6) (Table 2). Patient-05 and patient-07 were two representative cases with the confirmed best response of PR (Fig. 5).

Multivariate analysis indicated that liver metastasis was independent prognostic factors for PFS (Supplementary Table S3). Patients who had liver metastasis exhibited a median PFS of 5.6 months (95% CI 3.6–7.5) and median OS of 10.6 months (95% CI 5.8–15.4), while that for patients without liver metastatic lesions was NR (Supplementary Fig. S1). Similar significant mPFS (10.1 months vs 4.5 months, $P = 0.047$) and mOS (NR vs 5.4 months, $P = 0.0053$) benefits were

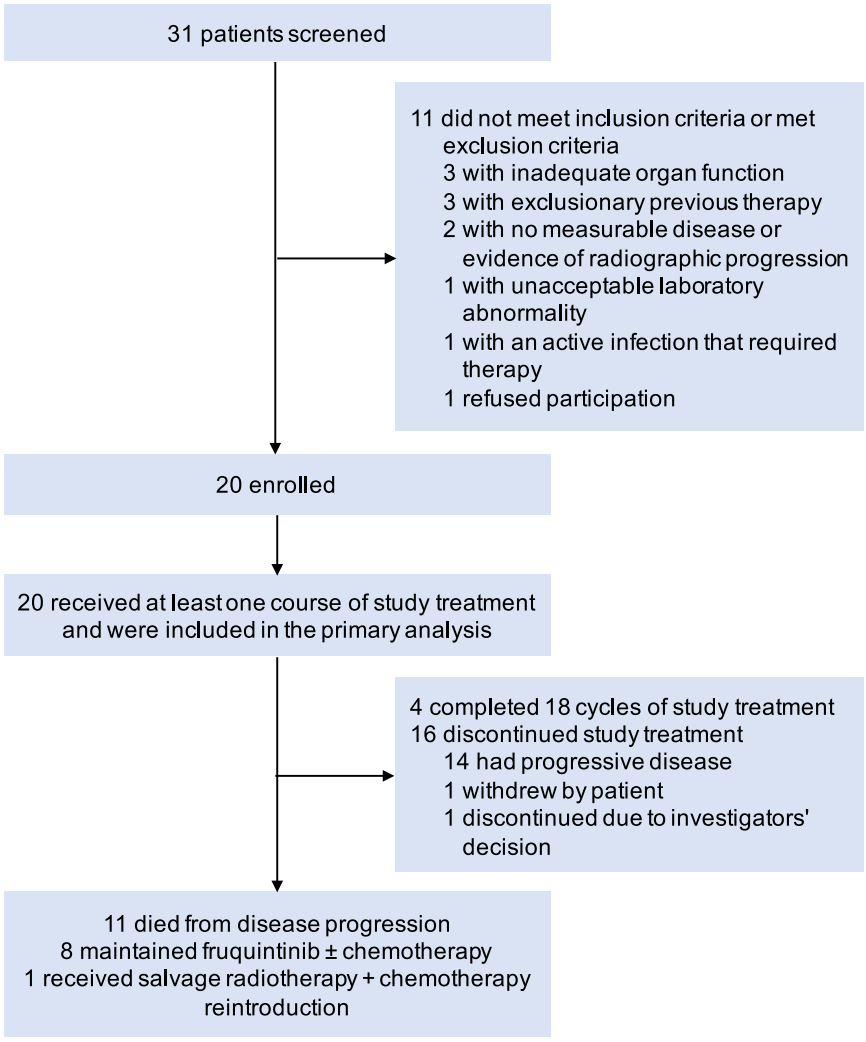

Fig. 1: CONSORT diagram of the study.

observed in patients with better ECOG PS score, but it was neither the independent prognostic factor for PFS nor for OS (Supplementary Table S3). Instead, the survival curves only showed non-significantly better trends in patients with previous radiotherapy or without prior anti-VEGF therapy (Supplementary Fig. S1).

Safety

Most patients (95%) experienced at least one treatment-related adverse event (TRAE) and the majority were grade 1 or 2 (Table 3). The most common TRAEs were decreased appetite (65%), fatigue (55%), albuminuria (55%) and fecal occult blood (55%). Grade 3–4 TRAEs were observed in 6 patients (30%), and the most common TRAEs were albuminuria (10%), fecal occult blood (10%), urine occult blood (10%), hypertension (5%), hyperglycemia (5%), liver dysfunction (5%), hand-foot skin reaction (HFSR, 5%), and hypothyroidism (5%).

TRAEs deemed by the investigator to be immune related AEs (irAEs) of any grade occurred in 8 (40%) patients and were serious in 2 patients (10%; grade 3 abnormal liver function (5%), and grade 3 hypertension and hyperglycemia (5%)). Most irAEs were grade 1–2. No treatment-related deaths occurred.

Dose reduction of fruquintinib was observed in one patient with grade 3 HFSR (5%). Two patients (10%) required one or more interruptions for study treatment. Owing to grade 3 hepatic dysfunction, one patient terminated tislelizumab ahead of disease progression. Another one refused further administration due to patient refusal. As of July 10, 2023, 4 patients completed 18 cycles of the study treatment and 3 continued to receive fruquintinib maintenance alone without PD. Sixteen patients (80%) discontinued the study treatment, of which 14 developed PD and 11 died from PD (Fig. 1).

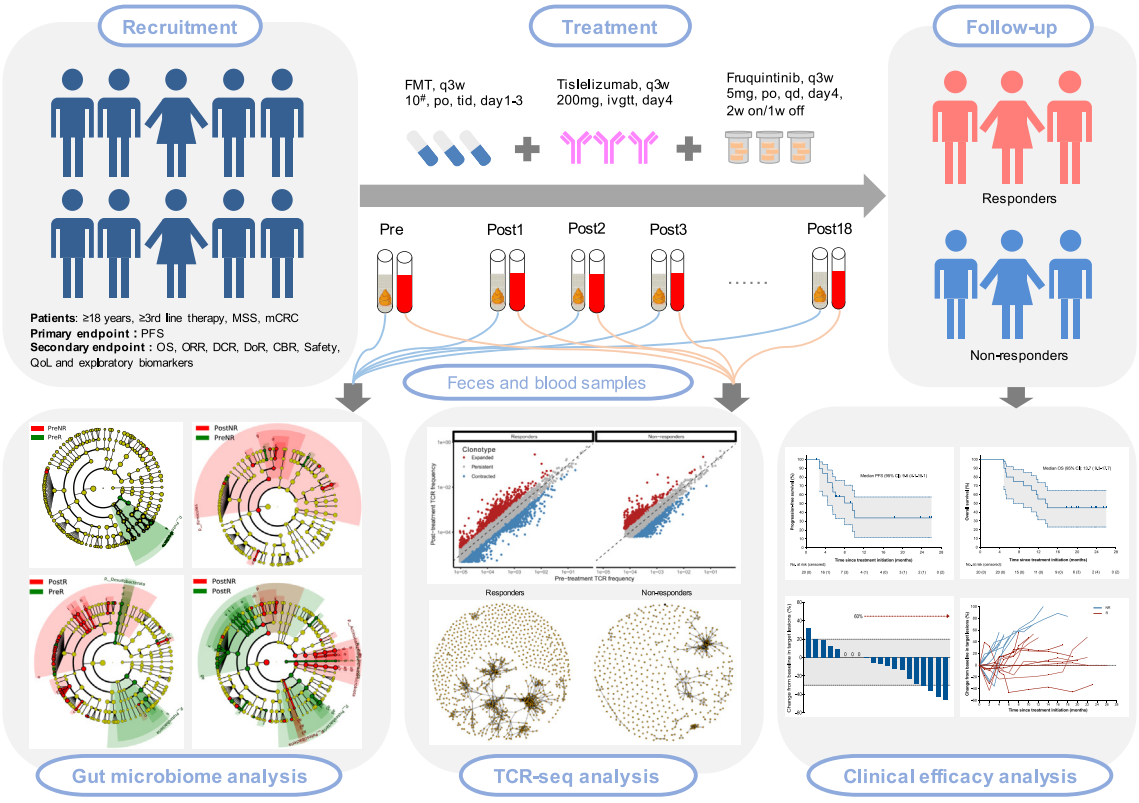

Fig. 2: Flowchart of the trial.

Stool 16S rDNA sequencing

A total of 116 fecal samples were collected during the course of study. From the samples, a total of 15,146,787 raw tags and 14,348,527 effective tags (mean length, 253 bp) were mapped to 6823 amplicon sequence variants (ASVs) (Supplementary Fig. S2A). The species composition of the samples was consistent with the composition characteristics of gut microbiota (Supplementary Fig. S2B). The rarefaction curves of operation taxonomy unit (OUT) richness reached a plateau and rank abundance curves of OTU distribution were long and flat (Supplementary Fig. S2C and D), indicating that our sequencing depth was sufficient and the community composition was uniform. No significant differences in alpha and beta diversity were observed in all baseline samples (Supplementary Fig. S3A–D). In terms of microbial composition of baseline samples, *Firmicutes* and *Bacteroidota* were the predominant phyla. *Proteobacteria* and *Actinobacteriota* were enriched in responders and non-responders, respectively (Supplementary Fig. S3E–G). High-abundance of *Proteobacteria* and low-abundance *Actinobacteriota* were associated with better survival outcomes (Supplementary Fig. S3K–P).

After identifying the signature of the gut microbiome in mCRC patients, we then explored what impacts study treatment would impose on the gut microbiome, and whether these perturbations would relate to clinical efficacy. Repeated fecal sampling at post-treatment was conducted. Significant differences in alpha and beta diversity were observed (Fig. 6A and B). *Proteobacteria* was increased at the phylum level in responders, while *Actinobacteriota* and *Patescibacteria* were significantly more abundant in non-responders (Fig. 6C–E). At the genus level, *Lachnospira, Lachnospiraceae_NK4A136_group, Roseburia, Clostridia_UCG-014, Enterobacter, Escherichia-Shigella, Clostridium_sensu_stricto_1, Eubacterium_eligens_group, Eubacterium_ruminantium_group,* and *Faecalibacterium* were observed significantly increased in responders, along with functional enrichment of important biological processes such as glycolysis, TCA cycle, amino acid metabolism, flagellar assembly and bacterial chemotaxis (Fig. 6F–H). Peptidoglycan biosynthesis was revealed to be a significantly enriched MetaCyc metabolic pathway associated with therapeutic response (Supplementary Fig. S4).

Combining taxonomic comparison results and gut microbiota network features, we constructed a response-prediction classifier for mCRC patients using random forest algorithm. Twenty microbial variables were selected as the optimal set, and the AUC reached 0.89 (Fig. 6I–K).

Characteristics	Patients (n = 20)
Age, median (range), years	62 (42–79)
Sex, n (%)	
Male	18 (90)
Female	2 (10)
ECOG PS, n (%)	
1	16 (80)
2	4 (20)
Primary tumor location, n (%)	
Left-side colon and rectum	14 (70)
Right-side colon	6 (30)
Type of metastasis, n (%)	
With liver metastasis	14 (70)
With lung metastasis	11 (55)
Previous treatment, n (%)	
Surgery	16 (80)
Chemotherapy	20 (100)
Radioactive intervention	9 (45)
Anti-EGFR therapy	4 (20)
Anti-VEGF/VEGFR therapy	14 (70)
Lines of prior cancer treatment	
2	9 (45)
≥3	11 (55)
Gene mutation status, n (%)	
KRAS/BRAF wild type	9 (45)
KRAS mutant type	7 (35)
BRAF mutant type	0
Unknown	4 (20)
MSI status	
MSS/pMMR	20 (100)
MSI-H/dMMR	0

Abbreviations: BRAF, V-raf murine sarcoma viral oncogene homolog B1; dMMR, mismatch repair deficiency; ECOG PS, Eastern Cooperative Oncology Group performance status; EGFR, epidermal growth factor receptor; KRAS, V-Ki-ras2 Kirsten rat sarcoma viral oncogene homolog; MSI, microsatellite instability; MSI-H, high microsatellite instability; MSS, microsatellite stable; pMMR, mismatch repair proficient; VEGF, vascular endothelial growth factor; VEGFR, vascular endothelial growth factor receptor.

Table 1: **Patient demographics and baseline characteristics.**

TCR sequencing

A total of 40 peripheral blood samples were collected and tested for the diversity, richness and clonality of TCR repertoire. However, no significant differences were found between responders and non-responders, and pre- and post-treatment (Supplementary Fig. S5). We then divided T cell clones into six categories according to TCR frequencies. The top thousand T cell clones occupied nearly 50% in each sample, the expanded clones and contracted clones were observed in responders and non-responders after treatment, but no novel T cell clones observed (Fig. 7A and B). Further clonotype clustering analysis showed that responders had more similar CDR3 cluster structures on expanded TCRs compared with non-responders (Fig. 7C and D). The length of the TCR CDR3β chain sequence in responders ranged from 10 to 17 amino acids. Or, to be more specific, the most common sequence length of the CDR3 β chain was 14-amino acids in clustered clones and 13-amino acids in non-clustered clones (Supplementary Fig. S6). The CDR3 amino acids of the clustered clones enriched in responders were characterized by low pI, small molecular weight and small average residue size (Fig. 7E).

The gene usage abundance of T-cell receptor beta variable (TRBV) and T-cell receptor beta joining (TRBJ) in clustered clones were confirmed to be similar in both groups (Supplementary Fig. S7). Previous study revealed that TCR sequence features influenced T cell fate.[26] Based on these TCR features, we trained a logistic regression model to evaluate whether the TCR features were effective in distinguishing the TCR sequences between the groups. The area under the curve (AUC) of the model reached 0.725 (Fig. 7F). The physicochemical features of hydropathicity, positive charge, secondary structure and codon diversity of the CDR3 middle region position were assessed to be associated with antigen-specific T cell response (Fig. 7G).

Discussion

In this clinical trial, which is, to our knowledge, the first prospective study to evaluate the antitumor activity and safety of FMT combined with tislelizumab and fruquintinib in MSS mCRC patients as a third-line or above therapy. Our results revealed that the combination of FMT plus tislelizumab and fruquintinib had promising antitumor activity with manageable toxicity profile.

For MSS mCRC patients without low-frequency or rare gene alterations who develop disease progression after failure of at least second-line therapy, the availability and efficacy of later-line treatments still fall short of what is needed. Rechallenging chemotherapy, considered a subsequent-line treatment, yielded a mOS of only 6–8 months, with a drop-out rate of more than 50%.[27,28] Similarly, regorafenib, TAS-102 or fruquintinib monotherapy, recommended as third-line treatments in clinical guidelines, demonstrated modest antitumor efficacy, with ORRs ranging from 1% to 4% and mPFS of 1.9–3.7 months.[5,15,29] Even worse, MSS mCRC patients are not considered an advantaged population for anti-PD-1/PD-L1 therapy due to the immunosuppressive TME. Therefore, the exploration of ICIs in refractory MSS mCRC has been full with challenges in the era of immunotherapy.

As mentioned above, regorafenib plus nivolumab reported in REGONIVO trial exhibited an ORR of 33% for MSS mCRC, with a mPFS of 7.9 month, opening the way for the combination of TKIs and ICIs.[13] Preclinical studies indicated that low dose anti-angiogenic therapy can normalize vasculature, increase tumor perfusion

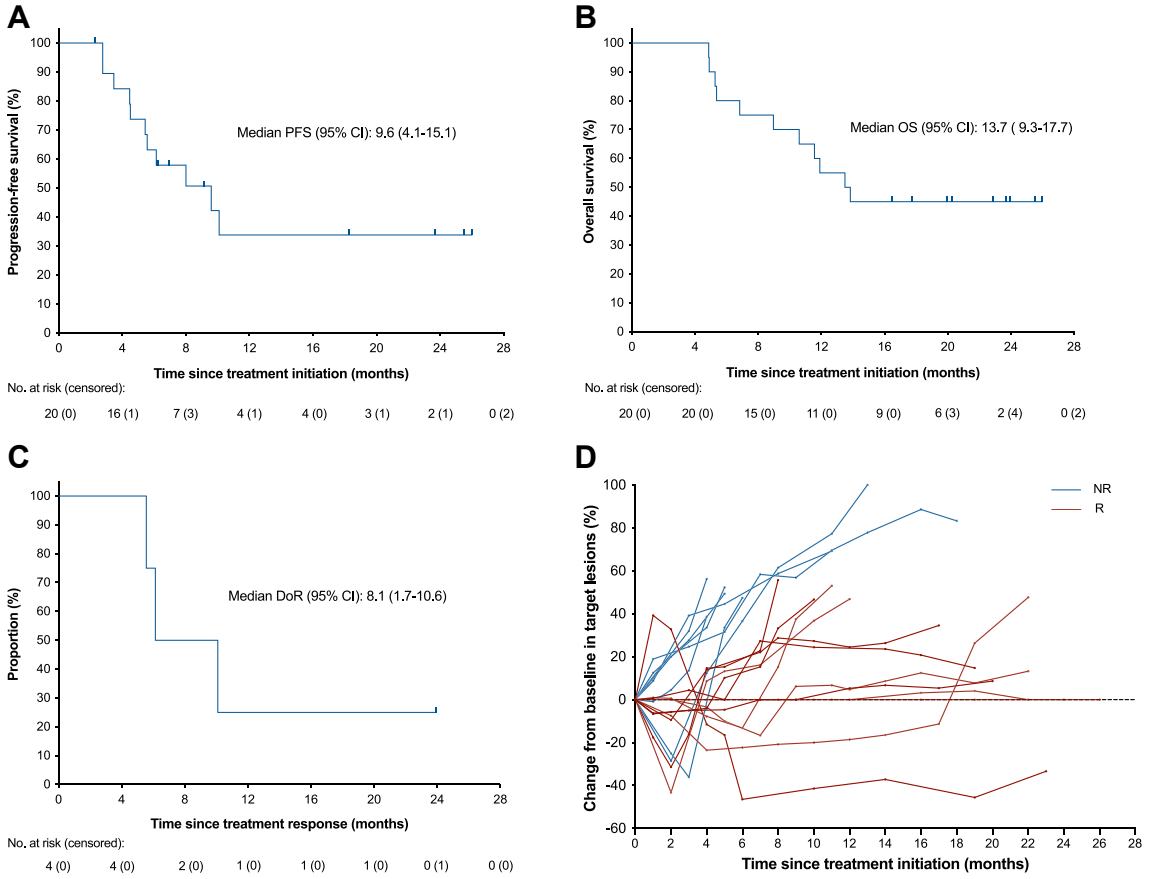

Fig. 3: Tumor response and Kaplan–Meier curves. (A) PFS and (B) OS were assessed in the ITT population (n = 20). (C) DoR was assessed in PR patients (n = 4). (D) Spider plot of tumor response in target lesions by month (Red line was defined as a patient who had survived without disease progression for more than 6 months). Data cut-off date for survival results was July 10, 2023. CI, confidence interval; DoR, duration of response; ITT, intention-to-treat; NR, non-responders; OS, overall survival; PFS, progression-free survival; R, responders.

and oxygenation, improve hypoxia, reduce tumor neoangiogenesis, promote chemokines release, increase the activation and infiltration of effector T-cells, decrease the maturation and accumulation of myeloid-derived suppressor cells, and polarize macrophages into M1-like phenotype, thereby reshaping the immunosuppressive TME towards a immunosupportive profile.[30] On the other hand, the feedback loops between ICIs-induced immune reprogramming and tumor vascular normalization reinforce each other to promote immune-mediated tumor eradication.[31]

Accumulating studies investigated the strategy of TKIs plus ICIs in the setting of MSS CRC and gained varying success. The LEAP-005 study, presented at the 2021 ASCO meeting, evaluated the antitumor activity of pembrolizumab and lenvatinib in MSS mCRC patients, resulting in an ORR of 22% but a mPFS of 2.3 months.[32] The phase II REGOMUNE trial, examined the efficacy of regorafenib with avelumab in pMMR CRC patients, showed an ORR of 0%, with a mPFS of 3.6 months.[33] In the recent phase II FRUIT trial, published in the 2023 ASCO-GI meeting, stereotatic body radiotherapy plus fruquintinib and tislelizumab as a later-line therapy in MSS mCRC showed improved mPFS of 8.5 months, with an ORR of 26%.[34] Local radiotherapy as an immunomodulator, can further enhance disease control on the basis of ICIs.

Likewise, as a promising additional method, FMT based on gut microbiome has also been reported to improve the antitumor immunity and promote response to ICIs.[19,35,36] Baruch et al. conducted a phase I trial to evaluate the combination of FMT and re-induction of ICIs in 10 patients with anti-PD-1-refractory metastatic melanoma, with 2 PR and 1 CR observed.[22] Davar's study showed that anti-PD-1 resistance can be overcome by inducing the gut microbiota perturbations via FMT, and that 6 of 15 melanoma patients obtained rapid and durable clinical benefit after the treatment of responder-derived FMT plus anti-PD-1.[23] Routy et al. found that FMT from epithelial cancer patients ameliorated the

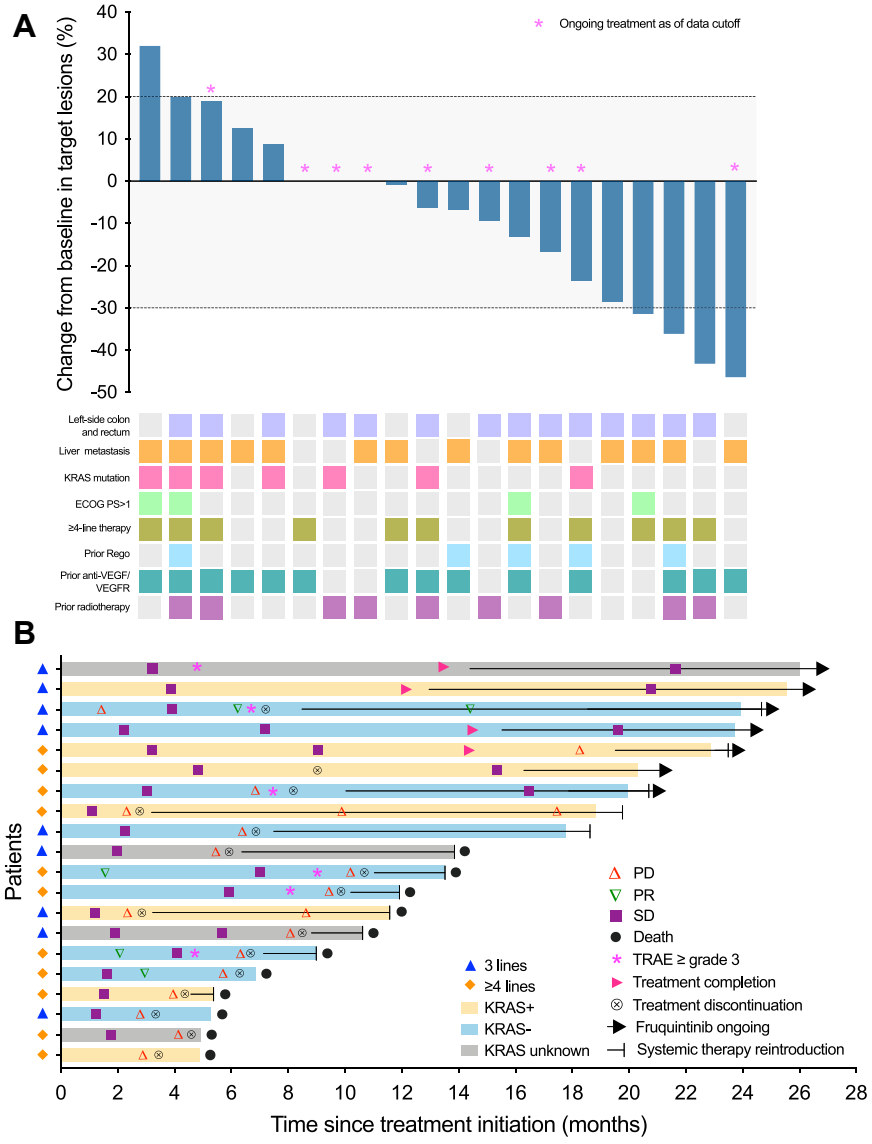

Fig. 4: Antitumor activity. (A) Waterfall plot showing the best percent change in the size of target lesions from baseline. The dashed lines at +20% and −30% indicate thresholds for PD and PR, respectively, according to RECIST 1.1. (B) Swimming plot for the onset of response, duration of response, and outcome. ECOG PS, Eastern Cooperative Oncology Group performance status; PD, progressive disease; PR, partial response; Rego, regorafenib; SD, stable disease; TRAE, treatment-related adverse event.

antitumor effects of PD-1-based immunotherapy in mice.[37] Huang's findings demonstrated that the combination of FMT and PD-1 inhibitor had superior survival outcome and tumor control than anti-PD-1 therapy or FMT alone in CRC tumor-bearing mice. FMT-increased *B. thetaiotaomicron*, *B. fragilis*, and FMT-decreased *B. ovatus* contributed to the enhanced efficacy of ICIs in CRC.[38]

In this trial, we enrolled MSS mCRC patients who had disease progression after prior at least second-line systemic treatment failure, with the hope that the new strategy of microbiota-based therapy combined with immunotherapy and anti-angiogenic target therapy would improve clinical outcomes. As expected, the survival benefit observed here was supported by the improved mPFS of 9.6 months (95% CI 4.1–15.1) and mOS of 13.7 months (95% CI 9.3–17.7) as well as higher ORR of 20% and DCR of 95%. Here, the PFS of 9.6 months is relatively conspicuous. But for the OS, we can only say that it is fine, not outstanding. Many factors are worth discussing. Already it is known that the past three years have been a challenging and difficult time

Variable	Patients (n = 20)
Confirmed best response, n (%)	
CR	0
PR	4 (20)
SD	15 (75)
PD	1 (5)
ORR, % (95% CI[a])	20 (5.7–43.7)
DCR, % (95% CI)	95 (75.1–99.9)
Median DoR (95% CI), months	8.1 (1.7–10.6)
CBR[b], % (95% CI)	60 (36.1–80.9)

Abbreviations: CBR, clinical benefited rate; CI, confidence interval; CR, complete response; DCR, disease control rate; DoR, duration of response; ORR, objective response rate; PD, progressive disease; PR, partial response; SD, stable disease. [a]Despite conservatism, the exact Clopper-Pearson method was used to compute binomial confidence intervals of each single rate due to the small sample size. [b]CBR was defined as PR + SD ≥ 6 months.

Table 2: **Efficacy outcomes.**

for all investigators conducting clinical trials and patients receiving appropriate treatments. And we thought that the repeated COVID-19 outbreaks and regional lockdowns from 2020 to 2023 were one of the main reasons that some patients were forced to terminate subsequent treatment. In contrast, we have a young patient with high tumor burden and KRAS G12D mutation enrolled for third-line treatment with a PFS of only 2.2 months, who insisted on returning to our cancer center for subsequent clinical management during the epidemic and is still alive after sixth-line treatment failure, with an OS of more than 24 months since his initial enrollment, highlighting the essentiality of standard whole-process management for clinical outcomes in mCRCs. After the normalization of the epidemic, better results deserve to be expected.

Consistent with previous findings, liver metastasis and high PS score were two independent risk factors associated with poor survival and prognosis.[14] In addition, we observed that a history of prior radiotherapy was associated with a trend towards better response for mCRC patients receiving subsequent immunotherapy-based systemic treatment. Evidence-based studies on the role of radiation therapy in immune response is growing. Radiotherapy, as an immunomodulator, has been reported to deeply reshape the TME by increasing tumor neoantigens release, activating innate immune pathways, improving effector T-cell infiltration, and enhancing antigen presentation.[39,40]

The regimen was well tolerated and there were no deaths attributed to AEs. The safety profiles were consistent with that noticed with ICIs and TKIs in CRC and other solid tumors, and no unexpected safety signals were observed. Most AEs were grade 1–2 and were manageable with standard-of-care interventions, including appetite loss, fatigue, hoarseness, hypertension, hypothyroidism, liver dysfunction, HFSR, diarrhea, bloating and pain. Grade 3 or worse AEs occurred in 6/20 (30%) patients, which is quite different from the recently published FRESCO-2 study, the change of the administration mode of fruquintinib from a 4-week regimen (3w on/1w off) to a 3-week regimen (2w on/1w off) may be largely responsible for the differences.[41] In a series of clinical

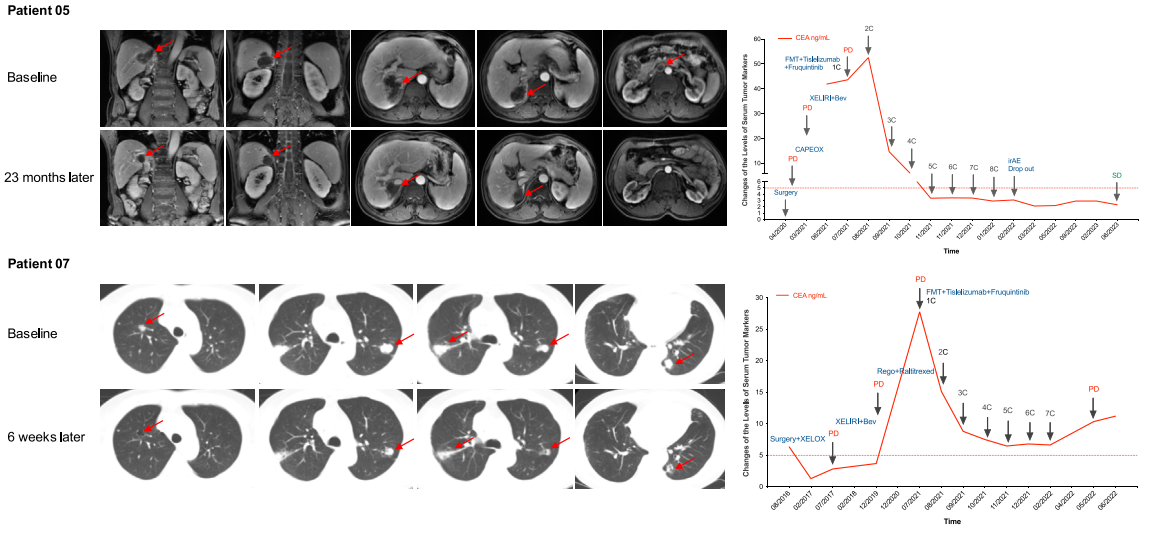

Fig. 5: Typical case presentation. Representative images of two patients and the dynamic changes of serum tumor markers. Bev, bevacizumab; C, cycle; CAPEOX/XELOX, capecitabine/oxaliplatin; CEA, carcinoembryonic antigen; FMT: fecal microbiota transplantation; irAEs: immune-related adverse events; XELIRI, capecitabine/irinotecan; PD, progressive disease; Rego, regorafenib; SD, stable disease.

		Patients (n = 20)
Any Grade TRAEs, No. (%)		19 (95)
Grade ≥3		6 (30)
Treatment suspension		2 (10)
Dose reduction		1 (5)
Death		0
Incidence rate	**Any Grade**	**Grade ≥3**
HFSR	5 (25)	1 (5)
Rash	4 (20)	0
Pruritus	3 (15)	0
Diarrhea	6 (30)	0
Bloating	4 (20)	0
Constipation	2 (10)	0
Ileus	3 (15)	0
Hypothyroidism	8 (40)	1 (5)
Hyperthyroidism	1 (5)	0
Liver dysfunction	5 (25)	1 (5)
Hypertension	7 (35)	1 (5)
Hyperglycemia	4 (20)	1 (5)
Weight loss	3 (15)	0
Fatigue	11 (55)	0
Decreased appetite	13 (65)	0
Hoarseness	8 (40)	0
Dry mouth	5 (25)	0
Mucositis oral	2 (10)	0
Periodontal disease	2 (10)	0
Epistaxis	8 (40)	0
FOBT positive	11 (55)	2 (10)
Albuminuria	11 (55)	2 (10)
Urine occult blood	7 (35)	2 (10)
Fever	3 (15)	0
Leukopenia	3 (15)	0
Thrombocytopenia	2 (10)	0
Hypoalbuminemia	2 (10)	0
Anemia	3 (15)	0
Hypokalemia	2 (10)	0
Hyponatremia	1 (5)	0
Headache	4 (20)	0
Musculoskeletal pain	2 (10)	0
Visual fatigue	1 (5)	0
Insomnia	2 (10)	0
Hypomnesis	1 (5)	0
Nausea	2 (10)	0
Vomiting	1 (5)	0
Cough	1 (5)	0

Abbreviations: TRAEs: treatment-related adverse events; HFSR: hand-foot skin reaction; FOBT, fecal occult blood test.

Table 3: **TRAEs.**

studies based on fruquintinib, we have also witnessed the exploration of different administration modalities of fruquintinib (Supplementary Table S4). Guo et al. compared fruquintinib 5 mg at a 3-week regimen with 3 mg at a continuous regimen and found that the former had better mPFS (6.9 m vs 4.2 m) and mOS (14.8 m vs 9.3 m) with a lower incidence of grade 3 or worse AEs (36.4% vs 59.1%) in mCRCs.[16] Indeed, in our clinical practice, the adjustment can not only keep pace with other clinical treatments, but also reduce the occurrence of AEs without significantly affecting the clinical efficacy, so as to improve the clinical treatment compliance of patients. Ethnic and regional differences, as well as different lifestyle and diet habits may also be non-negligible reasons for the discrepancy, given that CRC is a highly heterogeneous tumor. In brief, therapeutic strategies that improve survival without negatively affecting patients' quality of life are directions we have been exploring.

To identify potential biomarkers for predicting clinical response, screening suitable patients, optimizing treatment regimens and risk stratification, we performed gut microbiome analysis. Our results are generally consistent with previous reports on how gut microbiota and microbiota-derived or -mediated metabolites are involved in CRC carcinogenesis, progression and sensitivity to ICIs.[36,38,42] Comparison of post-treatment microbiota compositions demonstrated that responders had a higher relative abundance of the previously described as immunotherapy-favorable *Lachnospiraceae* family and a lower relative abundance of *Bifidobacterium*, which was reported to promote immune tolerance via T-reg cells.[22,43] The functional metabolic data showed that the responders up-regulated peptidoglycan biosynthesis, flagellar assembly and bacterial chemotaxis pathways.

Blockage of the antigen-presenting process within the tumor cells is a recognized mechanism of resistance to ICIs. A human FMT study in immunotherapy-refractory melanoma patients showed that microbiota-driven gut antigen presenting cells activation would yield increased intra-tumoral CD8+ T cell infiltration.[22] Multiple studies based on mouse models have also shown that gut microbiota intervention promoted infiltration of DCs into distant tumors, resulting in activation of T-helper 1 cells and cytotoxic CD8+ T cells.[37,44,45] Since the fecal microbiota was transplanted into the gut, it is reasonable to speculate that the immune activation cascade begins in the gut and subsequently migrates into the lymphatic system and peripheral circulatory system, and finally promoting the response to ICIs. To detect the peripheral immune cell-mediated antitumor immunity and cancer immunotherapy response, peripheral blood samples were collected and analyzed via TCR-seq. However, no differences of TCR repertoire were found. Through clonotype clustering analysis, we found the expanded TCRs showed the clustering characteristics of antigen-driven responses. In short, both beneficial gut microbiota and immunosupportive TME have

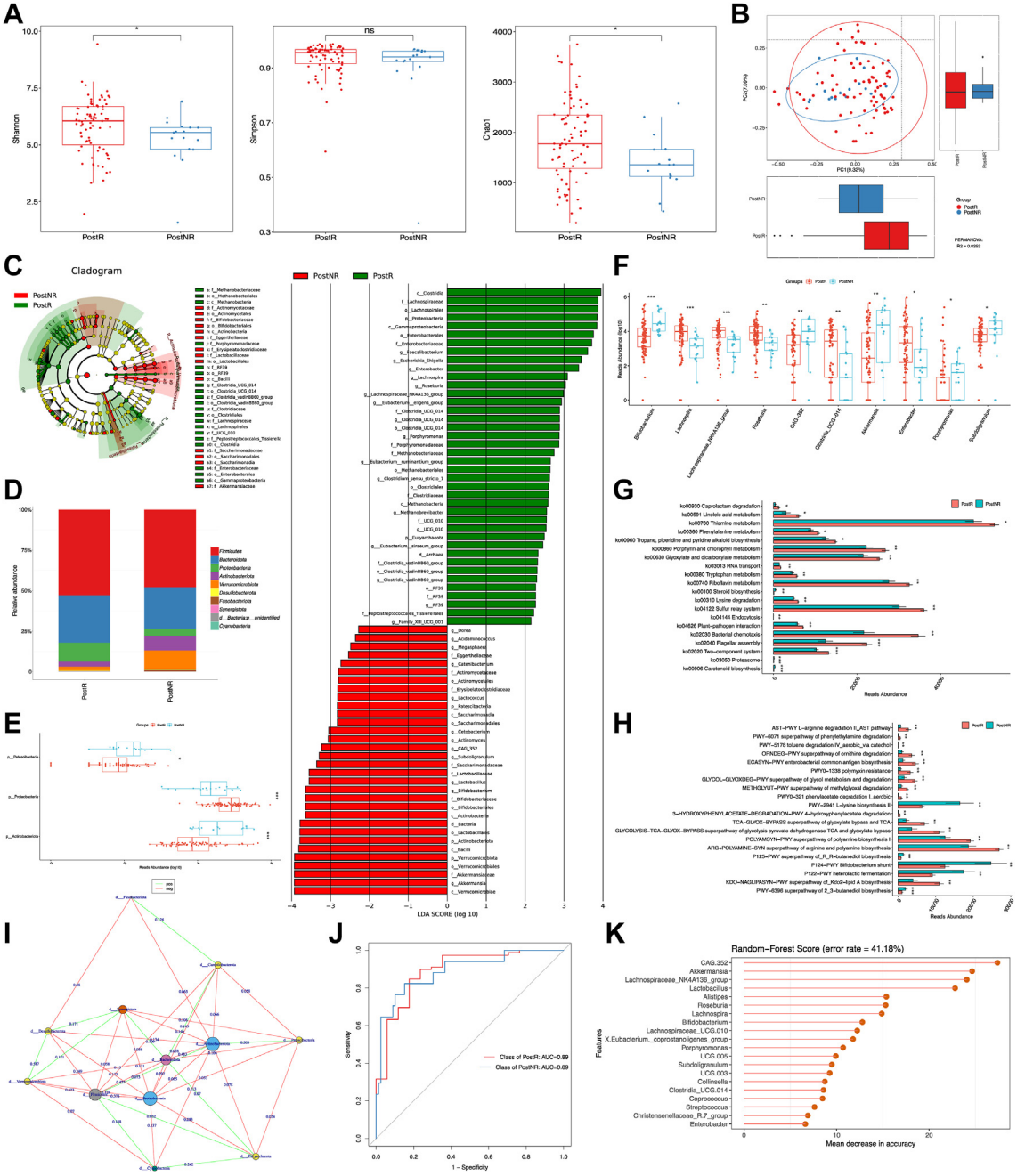

Fig. 6: The gut microbiome after study treatment in responders significantly differed from that in non-responders. (A) Alpha diversity indices as measured by Shannon index (P = 0.036), Simpson index (P = 0.18), and Chao1 index (P = 0.021), demonstrated significantly higher diversity and a trend towards higher unevenness in post-treatment fecal samples in responders than non-responders. (B) Beta diversity in post-treatment samples by response status was statistically significant in PCoA based on Bray Curtis distance (P = 0.0010). (C) Differentially abundant taxa analyzed by LefSe are projected as cladogram (left) and histogram (right). All listed taxa were significantly (Kruskal–Wallis test, P < 0.05; logarithmic LDA score >2) enriched for their respective groups (postNR, red and postR, green). (D) Stacked bar plot showing composition of common bacteria at the phylum level. (E–F) Box plot of the relative abundance of bacteria between groups at phylum and genus level, respectively. (G–H) Bar plots of the top 20 enriched differential KEGG and metabolic pathways in MetaCyc (postR, red and postNR, green). (I) Network analysis and visualization of interactions between species using Gephi. (J–K) Random forest classification for response based on the gut microbiome profiles at the genus level. ROC curve of the random forest classifier. Feature importance dot plot of the random forest classifier. *, P < 0.05; **, P < 0.01; ***, P < 0.001. AUC, area under the curve; KEGG, Kyoto Encyclopedia of Genes and Genomes; LDA, linear discriminant analysis; PCoA, principal coordinate analysis; PostR, post-treatment samples from responders; PostNR, post-treatment samples from non-responder; ROC, receiver operator characteristic.

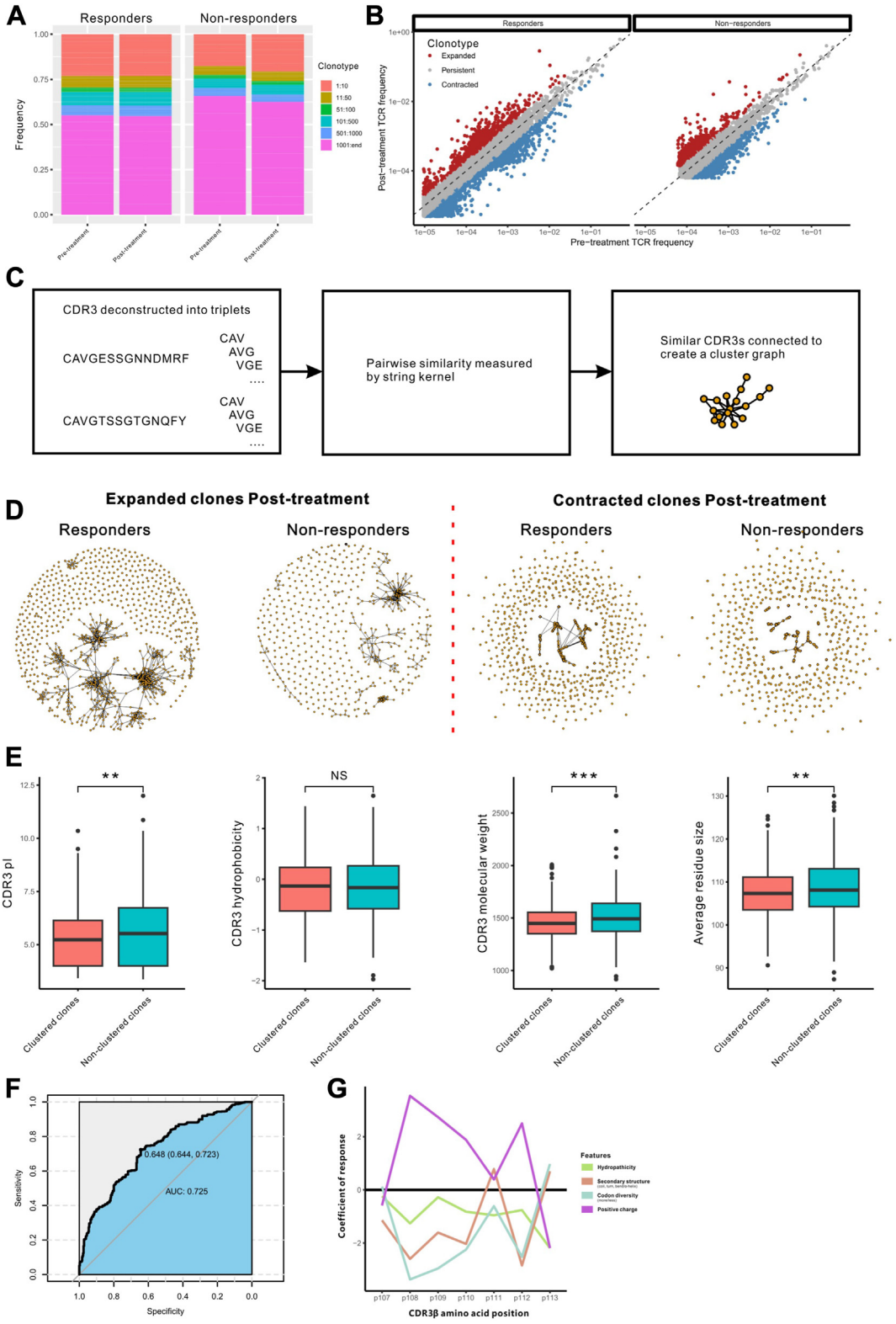

Fig. 7: The expanded TCRs in responders show more cluster structures. (A) The frequency of clonotypes distribution range in each sample. (B) Correlated clone sizes in PBMCs samples. Scatterplots of clonotypes size pre- and post-treatment in the top thousand clonotypes. Red indicates

immune-boosting effects, but neither is the only factor mediating the immune response. The optimal microbiota compositions, dosage forms, administration timing warrant further study yet.

Several limitations exist, including the small sample size, single-center, single-arm, and open-label study design. Although the gut microbiome and peripheral blood TCR analyses were performed, further molecular mechanism exploration and laboratory and clinical validation are lacking. Besides, due to the limited access to tissue samples, we did not analyze multiple immune-related gene sets at the histological level. Despite many inadequacies, the robust and better-than-expected response is encouraging and worthy of confirmation in a larger trial.

In summary, FMT combined with tislelizumab and fruquintinib showed encouraging anti-tumor efficacy and acceptable safety in refractory MSS mCRC patients after previous standard systemic therapies failure. A lower relative abundance of *Bifidobacterium* and a higher abundance of *Lachnospiraceae* in fecal samples and expanded TCR CDR3β clusters in peripheral blood appeared to be valuable classifiers for prognosis prediction and risk stratification. Future randomized controlled trials are needed to confirm these results.

Contributors

YSC performed study conception and design. WSZ, SBK, YC, JPX, ZT, LW, YPR, HQ and WS enrolled patients and collected data. YSC, SBK and LY conducted quality control and supervision; MA provided administrative and technical support for FMT; JL and LY contributed to the TCR-sequencing, analysis and interpretation of the data; WSZ did the statistical analysis and drafted the manuscript with the assistance and feedback of all other co-authors. All authors critically reviewed drafts of the manuscript and approved the final manuscript.

Data sharing statement

The study protocol is provided in the supplementary appendix. The datasets used and/or analyzed during the current study are available from the corresponding author on reasonable request.

Declaration of interests

The authors declare no conflicts of interest.

Acknowledgements

We thank the patients and their families, the study investigators, coordinators, and research staff. Tislelizumab was provided by BeiGene Co., Ltd. Capsulized FMT and 16S rDNA sequencing were provided and assisted by Jiangxi Shanxing Biotechnology Co., Ltd. We would also like to acknowledge Cuimin Wang for gut microbiome analysis.

Appendix A. Supplementary data

Supplementary data related to this article can be found at https://doi.org/10.1016/j.eclinm.2023.102315.

References

1 Sung H, Ferlay J, Siegel RL, et al. Global cancer statistics 2020: GLOBOCAN estimates of incidence and mortality worldwide for 36 cancers in 185 countries. *CA Cancer J Clin*. 2021;71(3):209–249.
2 Benson AB, Venook AP, Al-Hawary MM, et al. Colon cancer, version 2.2021, NCCN clinical practice guidelines in oncology. *J Natl Compr Canc Netw*. 2021;19(3):329–359.
3 Benson AB, Venook AP, Al-Hawary MM, et al. Rectal cancer, version 2.2022, NCCN clinical practice guidelines in oncology. *J Natl Compr Canc Netw*. 2022;20(10):1139–1167.
4 Biller LH, Schrag D. Diagnosis and treatment of metastatic colorectal cancer: a review. *JAMA*. 2021;325(7):669–685.
5 Grothey A, Van Cutsem E, Sobrero A, et al. Regorafenib monotherapy for previously treated metastatic colorectal cancer (CORRECT): an international, multicentre, randomised, placebo-controlled, phase 3 trial. *Lancet (London, England)*. 2013;381(9863):303–312.
6 Kuboki Y, Nishina T, Shinozaki E, et al. TAS-102 plus bevacizumab for patients with metastatic colorectal cancer refractory to standard therapies (C-TASK FORCE): an investigator-initiated, open-label, single-arm, multicentre, phase 1/2 study. *Lancet Oncol*. 2017;18(9):1172–1181.
7 Xu J, Kim TW, Shen L, et al. Results of a randomized, double-blind, placebo-controlled, phase III trial of trifluridine/tipiracil (TAS-102) monotherapy in Asian patients with previously treated metastatic colorectal cancer: the TERRA study. *J Clin Oncol*. 2018;36(4):350–358.
8 Andre T, Shiu KK, Kim TW, et al. Pembrolizumab in microsatellite-instability-high advanced colorectal cancer. *N Engl J Med*. 2020;383(23):2207–2218.
9 Finn RS, Qin S, Ikeda M, et al. Atezolizumab plus bevacizumab in unresectable hepatocellular carcinoma. *N Engl J Med*. 2020;382(20):1894–1905.
10 Larkin J, Chiarion-Sileni V, Gonzalez R, et al. Five-year survival with combined nivolumab and ipilimumab in advanced melanoma. *N Engl J Med*. 2019;381(16):1535–1546.
11 Le DT, Uram JN, Wang H, et al. PD-1 blockade in tumors with mismatch-repair deficiency. *N Engl J Med*. 2015;372(26):2509–2520.
12 Paz-Ares L, Luft A, Vicente D, et al. Pembrolizumab plus chemotherapy for squamous non-small-cell lung cancer. *N Engl J Med*. 2018;379(21):2040–2051.
13 Fukuoka S, Hara H, Takahashi N, et al. Regorafenib plus nivolumab in patients with advanced gastric or colorectal cancer: an open-label, dose-escalation, and dose-expansion phase ib trial (REGONIVO, EPOC1603). *J Clin Oncol*. 2020;38(18):2053–2061.
14 Wang F, He MM, Yao YC, et al. Regorafenib plus toripalimab in patients with metastatic colorectal cancer: a phase Ib/II clinical trial and gut microbiome analysis. *Cell Rep Med*. 2021;2(9):100383.
15 Li J, Qin S, Xu RH, et al. Effect of fruquintinib vs placebo on overall survival in patients with previously treated metastatic colorectal cancer: the FRESCO randomized clinical trial. *JAMA*. 2018;319(24):2486–2496.
16 Guo Y, Zhang W, Ying J, et al. Phase 1b/2 trial of fruquintinib plus sintilimab in treating advanced solid tumours: the dose-escalation and metastatic colorectal cancer cohort in the dose-expansion phases. *Eur J Cancer*. 2023;181:26–37.
17 Matson V, Fessler J, Bao R, et al. The commensal microbiome is associated with anti-PD-1 efficacy in metastatic melanoma patients. *Science (New York, NY)*. 2018;359(6371):104–108.
18 Sun JY, Yin TL, Zhou J, Xu J, Lu XJ. Gut microbiome and cancer immunotherapy. *J Cell Physiol*. 2020;235(5):4082–4088.
19 Gopalakrishnan V, Spencer CN, Nezi L, et al. Gut microbiome modulates response to anti-PD-1 immunotherapy in melanoma patients. *Science (New York, NY)*. 2018;359(6371):97–103.
20 Huang J, Liu D, Wang Y, et al. Ginseng polysaccharides alter the gut microbiota and kynurenine/tryptophan ratio, potentiating the antitumour effect of antiprogrammed cell death 1/programmed cell

expanded clones (≥2-fold increase), blue indicates contracted clones (≥2-fold decrease). (C) Diagram describes the construction process of similar CDR3 sequences. (D) Clusters formed from CDR3 sequences of expanded clones and contracted clones. (E) CDR3 amino acid physicochemical properties from clustered clones and non-clustered clones in responders. (F) Estimation of the specificity and sensitivity by the logistic regression model with ROC curve. (G) The line plot of the correlation between T cell response score and amino acid physicochemical features of CDR3 middle region position. **, $P < 0.01$; ***, $P < 0.001$. CDR, complementarity-determining region; PBMC, Peripheral blood mononuclear cells; ROC, receiver operating characteristic.

death ligand 1 (anti-PD-1/PD-L1) immunotherapy. *Gut*. 2022;71(4):734–745.
21 Sivan A, Corrales L, Hubert N, et al. Commensal Bifidobacterium promotes antitumor immunity and facilitates anti-PD-L1 efficacy. *Science (New York, NY)*. 2015;350(6264):1084–1089.
22 Baruch EN, Youngster I, Ben-Betzalel G, et al. Fecal microbiota transplant promotes response in immunotherapy-refractory melanoma patients. *Science (New York, NY)*. 2021;371(6529):602–609.
23 Davar D, Dzutsev AK, McCulloch JA, et al. Fecal microbiota transplant overcomes resistance to anti-PD-1 therapy in melanoma patients. *Science (New York, NY)*. 2021;371(6529):595–602.
24 Lee A, Keam SJ. Tislelizumab: first approval. *Drugs*. 2020;80(6):617–624.
25 Zhang L, Geng Z, Hao B, Geng Q. Tislelizumab: a modified anti-tumor programmed death receptor 1 antibody. *Cancer Control*. 2022;29:10732748221111296.
26 Lagattuta KA, Kang JB, Nathan A, et al. Repertoire analyses reveal T cell antigen receptor sequence features that influence T cell fate. *Nat Immunol*. 2022;23(3):446–457.
27 Suenaga M, Mizunuma N, Matsusaka S, et al. Phase II study of reintroduction of oxaliplatin for advanced colorectal cancer in patients previously treated with oxaliplatin and irinotecan: RE-OPEN study. *Drug Des Devel Ther*. 2015;9:3099–3108.
28 Yang Q, Huang Y, Jiang Z, et al. Rechallenge of oxaliplatin-containing regimens in the third- or later-line therapy for patients with heavily treated metastatic colorectal cancer. *OncoTargets Ther*. 2018;11:2467–2473.
29 Yoshino T, Mizunuma N, Yamazaki K, et al. TAS-102 monotherapy for pretreated metastatic colorectal cancer: a double-blind, randomised, placebo-controlled phase 2 trial. *Lancet Oncol*. 2012;13(10):993–1001.
30 Huang Y, Goel S, Duda DG, Fukumura D, Jain RK. Vascular normalization as an emerging strategy to enhance cancer immunotherapy. *Cancer Res*. 2013;73(10):2943–2948.
31 Khan KA, Kerbel RS. Improving immunotherapy outcomes with anti-angiogenic treatments and vice versa. *Nat Rev Clin Oncol*. 2018;15(5):310–324.
32 Gomez-Roca C, Yanez E, Im S-A, et al. LEAP-005: a phase II multicohort study of lenvatinib plus pembrolizumab in patients with previously treated selected solid tumors—results from the colorectal cancer cohort. *J Clin Oncol*. 2021;39(3_suppl):94.
33 Cousin S, Cantarel C, Guegan JP, et al. Regorafenib-avelumab combination in patients with microsatellite stable colorectal cancer (REGOMUNE): a single-arm, open-label, phase II trial. *Clin Cancer Res*. 2021;27(8):2139–2147.
34 Yuan X, Zhang M, Hou H. Fruquintinib combined with tislelizumab and SBRT as a later-line therapy in microsatellite stability (MSS) metastatic colorectal cancer (mCRC): results from the FRUIT trial. *J Clin Oncol*. 2023;41(4_suppl):150.
35 Gopalakrishnan V, Helmink BA, Spencer CN, Reuben A, Wargo JA. The influence of the gut microbiome on cancer, immunity, and cancer immunotherapy. *Cancer Cell*. 2018;33(4):570–580.
36 Xu X, Lv J, Guo F, et al. Gut microbiome influences the efficacy of PD-1 antibody immunotherapy on MSS-type colorectal cancer via metabolic pathway. *Front Microbiol*. 2020;11:814.
37 Routy B, Le Chatelier E, Derosa L, et al. Gut microbiome influences efficacy of PD-1-based immunotherapy against epithelial tumors. *Science (New York, NY)*. 2018;359(6371):91–97.
38 Huang J, Zheng X, Kang W, et al. Metagenomic and metabolomic analyses reveal synergistic effects of fecal microbiota transplantation and anti-PD-1 therapy on treating colorectal cancer. *Front Immunol*. 2022;13:874922.
39 Jagodinsky JC, Harari PM, Morris ZS. The promise of combining radiation therapy with immunotherapy. *Int J Radiat Oncol Biol Phys*. 2020;108(1):6–16.
40 Mondini M, Levy A, Meziani L, Milliat F, Deutsch E. Radiotherapy-immunotherapy combinations–perspectives and challenges. *Mol Oncol*. 2020;14(7):1529–1537.
41 Dasari A, Lonardi S, Garcia-Carbonero R, et al. Fruquintinib versus placebo in patients with refractory metastatic colorectal cancer (FRESCO-2): an international, multicentre, randomised, double-blind, phase 3 study. *Lancet (London, England)*. 2023;402(10395):41–53.
42 Coker OO, Liu C, Wu WKK, et al. Altered gut metabolites and microbiota interactions are implicated in colorectal carcinogenesis and can be non-invasive diagnostic biomarkers. *Microbiome*. 2022;10(1):35.
43 Verma R, Lee C, Jeun EJ, et al. Cell surface polysaccharides of Bifidobacterium bifidum induce the generation of Foxp3(+) regulatory T cells. *Sci Immunol*. 2018;3(28).
44 Tanoue T, Morita S, Plichta DR, et al. A defined commensal consortium elicits CD8 T cells and anti-cancer immunity. *Nature*. 2019;565(7741):600–605.
45 Vetizou M, Pitt JM, Daillere R, et al. Anticancer immunotherapy by CTLA-4 blockade relies on the gut microbiota. *Science (New York, NY)*. 2015;350(6264):1079–1084.